E. W. Smith and K. J. Pascoe†*

Biaxial Fatigue of a Glass-Fibre Reinforced Composite. Part 2: Failure Criteria for Fatigue and Fracture

REFERENCE Smith, E. W. and Pascoe, K. J., **Biaxial fatigue of a glass-fibre reinforced composite. Part 2: failure criteria for fatigue and fracture**, *Biaxial and Multiaxial Fatigue*, EGF 3 (Edited by M. W. Brown and K. J. Miller), 1989, Mechanical Engineering Publications, London, pp. 397–421.

ABSTRACT The biaxial monotonic and fatigue strength properties of a woven roving glass reinforced polyester composite have been established using flat cruciform-shaped specimens. The results were compared with various earlier fracture criteria for anisotropic material.

A failure criterion has been proposed whose application depends only on values of the principal elastic constants, a uniaxial strength, and the shear strength parallel to a fibre plane. This criterion describes reasonably the failure surface for in-plane reversed fatigue loading and in-plane monotonic loading. It compares well with failure surfaces obtained from available 'distortional energy' and tensor-based failure criteria.

Introduction

Failure criteria evolved for anisotropic materials date back to the 1930s (1), when attempts were made to quantify the directional properties of wood. Early failure criteria applied specifically to fibre reinforced materials considered that the fibres carry tensile loads and the matrix transmits compressive and shear loads. Later criteria of more general character, and based on distortional energy (von Mises–Hencky), were developed from a theory of Hill (2) originally proposed for anisotropic metals. Development of 'distortional energy' criteria has progressed to the point where tensor methods are used to manipulate the resulting failure equation, as many as ten strength components being required to explain the plane stress state.

In the second part of this paper one of the generalised tensor criteria, that of Tsai and Wu (3), is considered and compared with the experimental complex strength data of the test grp described in Part I. Shortcomings, which are apparent, can be explained by the fact that the actual failure surface must circumscribe volumes with differing failure mechanisms. Observation of the fatigue behaviour of the test grp as described in Part I has led to ideas on the development of a failure criterion based on the interaction of normal stresses and shear on the fibre plane.

* Department of Production Technology, Massey University, Palmerston North, New Zealand.
† University Engineering Department, Cambridge, UK.

Notation

E_1, E_2	Elastic moduli in directions of fibre axes
EQ	Equibiaxial strength in 1–2 plane
$F_1, \ldots, F_6$	Strength tensors of 2nd rank
$F_{11}, \ldots, F_{66}$	Strength tensors of 4th rank
$F_{111}, \ldots, F_{666}$	Strength tensors of 6th rank
$K_1, \ldots, K_6$	Strength constants
n	Interaction exponent
N_f	Fatigue life (cycles)
$S_{45}, S^{\pm}_{45}$	Shear strength on plane at 45 degrees to fibre axes
$S, S^{\pm}, S_{12}$	Shear strengths in directions of fibre axes
U_F	Strain energy to cause failure
W, W'	Tensile and compressive strengths along 45 degree fibre axis
X, X'	Tensile and compressive strengths along 0 degree fibre axis
Y, Y'	Tensile and compressive strengths along 90 degree fibre axis
α, β, γ	Interaction factors
$\dot{\varepsilon}_{min}$	Minimum strain range accumulation rate
θ	Off-axis angle
λ	Load ratio (σ_x/σ_y)
ν	Poisson's ratio
ν_{12}, ν_{21}	Poisson's ratio in directions of fibre axes
σ	Applied maximum principal stress
$\sigma_1, \sigma_2, \sigma_6$	Normal stresses and shear stress in directions of fibre axes
σ_f	Component of tensile stress normal to fibre
σ_x, σ_y	Applied and principal stresses
$\overline{\sigma}_c$	Failure strength
$\overline{\sigma}_{rF}$	Failure strength due to shear degradation
$\overline{\sigma}_{uF}$	Failure strength due to rectilinear cracking
τ_f	Shear stress component along fibres
τ_{12}	Shear stress in directions of fibre axes

Review of anisotropic failure criteria

Various relationships have been proposed to correlate the variation of strength of anisotropic materials with multiaxiality of stress and directions of stress relative to the principal axes of anisotropy. There are two broad approaches – empirical and mechanistic. The empirical approach attempts to predict strength at failure from a mathematical model. The basis for the model does not depend on the constituent make-up of the composite and, indeed, can be the same for macroscopically different materials. This approach takes no account of the modes of failure. The mechanistic approach attempts to predict strength from the properties and failure characteristics of the constituent materials and their interrelationship with each other. This approach requires a careful study of the modes of failure of the composite and how the constituent materials contribute towards strength.

Empirical criteria

The empirical approach has been developed over the past 40 years or so, and most of the criteria can be seen to be adaptations of the quadratic 'distortional energy' theory of isotropic materials. The empirical failure criteria for in-plane uniaxial and biaxial loading are summarised in the Appendix. Theories have evolved to make use of tensor manipulation of the rotation of fibre and load axes, and early empirical criteria can be shown to be particular cases of the fourth-rank tensor criterion of Tsai and Wu (3). F_1, F_2, F_{11}, and F_{22} can be ascertained from measurements of uniaxial strength, and F_{66} from a measurement of shear strength. There are a number of combined stress states any of which may be used to establish a value of F_{12}. Furthermore, though the criteria of Puppo and Evensen (4), Gol'denblat and Kopnov (5), Ashkenazi (6), and Wu and Sheublein (7) are more intricate, they will reduce, by material symmetry and simplification to the six strength component form of Tsai and Wu, viz

$$F_1\sigma_1 + F_2\sigma_2 + F_{11}\sigma_1^2 + 2F_{12}\sigma_1\sigma_2 + F_{22}\sigma_2^2 + F_{66}\sigma_6^2 = 1 \qquad (1)$$

Tsai and Wu detailed three specific cases as alternatives for determining F_{12}, viz. use of the 45 degree off-axis uniaxial strength ($\lambda = 0$, $\theta = 45$ degrees), the equibiaxial strength ($\lambda = 1$) and the 45 degree shear strength ($\lambda = -1$, $\theta = 45$ degrees). Both Gol'denblat and Kopnov and Ashkenazi determined F_{12} from the uniaxial off-axis strength, but Tsai and Wu, with further emphasis from Wu (8) showed that the determination of F_{12} in this way is critical and small errors in the assessment of the 45 degree off-axis strength can give disproportionately large errors in F_{12}. Wu also showed that the optimum biaxial ratio for determining F_{12} depends on the sign of F_{12} itself and on the extent of experimental scatter. He considered the use of either the equibiaxial strength or the 45 degree shear strength to be best.

Having determined the values of the tensor components for failure of a particular material from six separate tests as outlined above, the applicability of the criterion can be judged by the degree to which it fits experimental data for other loading conditions. Owen and co-workers, e.g. (9)–(11), have applied a number of the fourth-order tensor criteria to static and fatigue data from uniaxial off-axis and biaxial (cylinders subject to internal pressure and axial load) experiments with various types of reinforcement.

A greater degree of fit could be expected using the criterion of Wu and Scheublin (7) which uses sixth-order tensors. However, determination of the tensor components requires a large number of experimental tests – sufficient in fact to determine the 'best-fit' criterion by numerical methods. Tennyson *et al.* (12), using the optimum biaxial ratio to determine F_{12}, compared the quadratic (fourth order) and cubic (sixth order) representation of the tensor polynomial for a series of cylinders laid up at various off-axis fibre angles and subject to internal pressure. Their experimental comparisons were of particular significance because none of the pertinent experimental data had been used to establish the strength components. They found that the cubic form gave a better fit to the experimental data and that the quadratic form tended to be conservative.

At the same time there are conflicting views which favour a simplified approach, at least for in-plane loading, with the use of the quadratic tensor criteria and F_{12} specified more strictly. Narayanaswami and Adelman **(13)** suggested $F_{12} = 0$ is sufficiently accurate for most engineering applications; they came to this conclusion by applying the theory to uniaxial off-axis experimental data. Tsai and Hahn **(14)** proposed establishing F_{12} by assuming that the two-dimensional failure boundary will be a distortion of the von Mises ellipse. Then

$$F_{12} = -\tfrac{1}{2}\sqrt{(F_{11} \cdot F_{22})} \tag{2}$$

Suffice it to say that the strength components of the ideal failure criterion should be capable of being evaluated from only 'simple' tests and material properties. An exhaustive review of the literature published on applying, comparing, and using the tensor-based criteria is not attempted here, but it is intended to show that there are conflicting views. The empirical criteria are just that; they do not purport to give any understanding or meaning to the failure strengths, they give a fit to the available experimental data (or sometimes not) and nothing more. A move must be made towards basing criteria on the mechanics and mechanisms of failure. The tensor polynomial equations can cope with changes in failure mode only by becoming mathematically more complex, and even then they will be unable to predict or follow an abrupt change in mode. Their development would appear to be limited.

Mechanistic criteria

The failure criteria which use a mechanistic approach have considered mainly the micromechanisms of static and fatigue failure in unidirectional fibre laminae and laminates; only limited study has been made of multidirectional, woven, or random fibre lay-ups. The micro-mechanisms of lamina failure for even the simplest unidirectional reinforcement are difficult to define explicitly. Any of a number of modes may contribute towards failure, e.g., debonding of fibres, matrix cracking, matrix void growth, delamination, fibre buckling, fibre pull-out, and/or fibre failure. However, the following three modes of failure are those that have been described most in mechanistic criteria.

(i) Fibre failure.
(ii) Matrix failure.
(iii) Fibre/matrix interface breakdown.

These may be of tensile, compressive, or shearing nature. Each mode may be considered to contribute to failure independently, or interact together, either linearly, as a quadratic relationship or as some complex interrelationship.

Puck and Schneider (**15**) recognised three stress systems contributing to failure – longitudinal stresses, transverse stresses, and longitudinal/transverse shear stresses (all with respect to the fibre direction). Fibre failure was dictated by longitudinal stress alone, matrix failure by a quadratic expression involving all three stress systems, and adhesive failure of the interface by a quadratic involving transverse and shear stresses. The three modes were considered to act independently to cause laminate failure, i.e., failure occurs when any one of the three equations predicts it.

Meanwhile, Sims and Brogdon (**16**), Hashin and Rotem (**17**) and Hashin (**18**) have proposed fatigue failure criteria. The latter based their theory on the two separate modes of fibre failure and matrix failure. For the plane stress situation both modes are described by a quadratic – the fibre mode is dictated by longitudinal and shear stresses, the matrix mode by transverse and shear stresses. Sims and Brogdon also took into account the fibre/matrix interface. However, in each case the modes were modelled separately and behaved independently. Hashin pointed out that mode separation is an idealisation, especially at mode intersection points on the failure surface where small domains will occur in which two modes are operative simultaneously.

Sanders *et al.* (**19**) have suggested that interaction does occur. In multidirectional laminates they observed three layer failure modes and a less significant delamination mode. The layer modes were a strain-dependent tensile mode, a buckling-related compressive mode, and a shear mode. Biaxial tests suggest that interaction may be strain-level dependent. They proposed interaction between the layer tension and layer shear modes of a quadratic form and between the layer compression and layer shear modes of a simpler linear form.

Representation of failure surfaces

The complete failure surface for an isotropic material, such as a laminate, subjected to in-plane loading, is three-dimensional and, strictly, should be represented as an envelope drawn on orthogonal σ_1, σ_2, τ_{12} axes. Graphical representation is tedious and, unless adequate construction lines are presented, the surface and position of failure points may not be readily apparent.

Ashkenazi (**6**) constructed the failure surface in a number of steps. Gol'denblat and Kopnov (**5**) only represented the surface as lines of constant load ratio. Owen and Found (**20**) avoided three-dimensional constructions by drawing the projection or the intersection of the failure surface onto the $\tau_{12} = 0$ plane. This form of presentation is unambiguous and is useful to compare different criteria, but it does not show a direct representation as required by the design engineer. Smith and Pascoe (**21**) have also got away from the three-dimensional view by rotating the principal stress axes and drawing failure ellipses for fixed fibre angles.

In this presentation the various failure surfaces have been represented as 2-D plots (Figs 1–4 and 6), except in one case where, as an example, the full failure surface has been drawn (Fig. 5(a)). For zero mean stress fatigue loading failure plots are constructed using only half of the σ_1/σ_2 plane as differentiation between tension and compression is not necessary. However, the whole σ_1/σ_2 plane is required for monotonic loading where tensile and compressive strengths may not be equal. In the case of the 3-D plot of Fig. 5(a) lines of fixed load ratios (+1, +0.5, 0, −0.5 and −1) and fixed fibre angles (0 and 90 degrees, 22½ degrees, and 45 and 135 degrees) are shown; the same information is shown as 2-D plots in Fig. 5(b).

Application of available strength criteria

Fatigue failure

When the criterion of Tsai and Wu is applied to fatigue testing with zero mean loading, as for the programme described in Part I, the second rank tensors, F_1 and F_2, are zero. Hence equation (1) reduces to

$$F_{11}\sigma_1^2 + 2F_{12}\sigma_1\sigma_2 + F_{22}\sigma_2^2 + F_{66}\tau_{12}^2 = 1 \quad (3)$$

Using equation (3), the failure ellipse for fatigue of the test laminate in 10^5 cycles is shown in Fig. 1. Two semi-ellipses are drawn, one with F_{12} derived from the equi-biaxial state, and the other with F_{12} derived from the 45 degree shear strength. Values of the fourth rank tensors in units of $(\text{MPa})^{-2}$ for 10^5 cycles are

$$F_{11} = 0.145 \times 10^{-3}$$
$$F_{22} = 0.169 \times 10^{-3}$$
$$F_{66} = 2.5 \times 10^{-3}$$

with

$$F_{12} = -0.042 \times 10^{-3}$$

from the equibiaxial strength and

$$F_{12} = -0.0025 \times 10^{-3}$$

from the 45 degree shear strength.

The influence of a more negative F_{12} is to pull the surface in the direction of increasing strength for $\lambda = +1$ and conversely to flatten it for negative load ratios. Neither the equibiaxial strength nor the 45 degree shear strength basis results in a good fit to the experimental data in *both* negative and positive load ratio quadrants. Equibiaxial strength would prove to be the better of the two, but even so, the form of the distortional energy basis would appear to be lacking. Using the 45 degree off-axis uniaxial strength to establish F_{12} would give $F_{12} = -1.23 \times 10^{-3}$, which violates the stability condition $F_{ii}F_{jj} - F_{ij}^2 \geqslant 0$

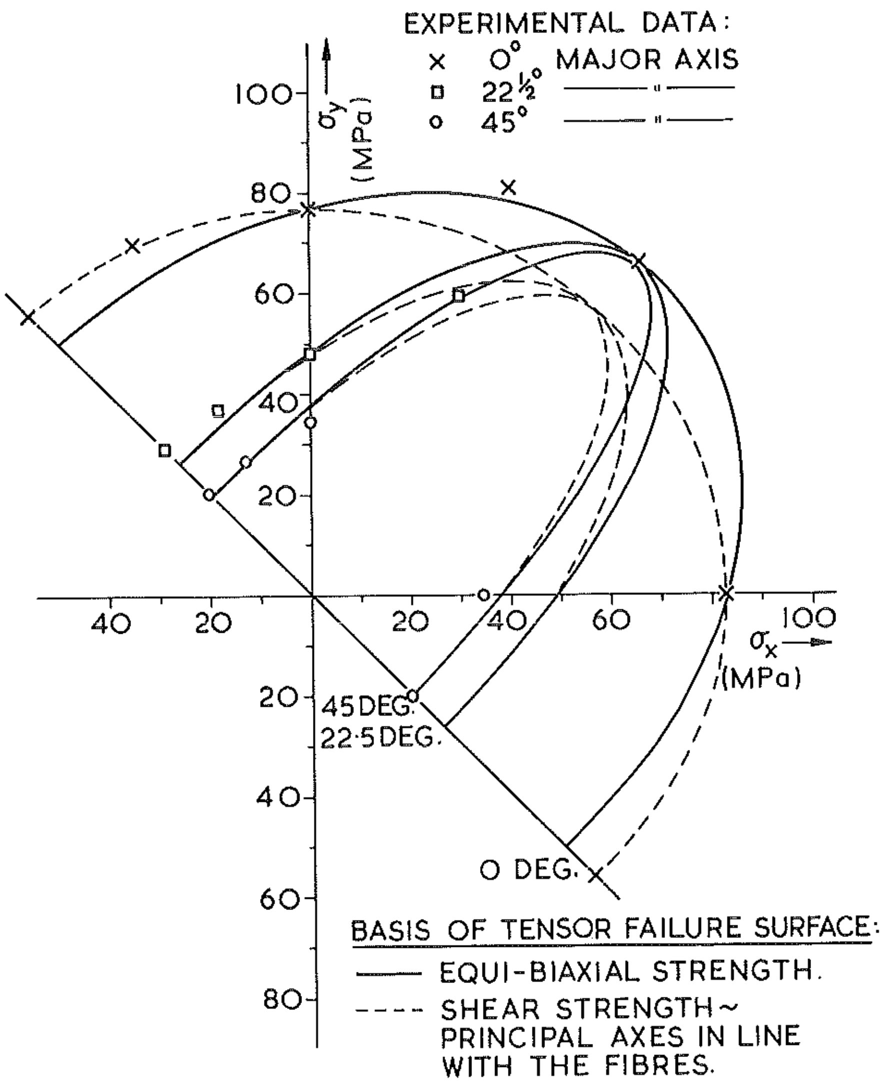

Fig 1 Failure envelopes for fatigue failure at 10^5 cycles based on the tensor criterion of Tsai and Wu (3). Drawn as 2-D plots for fibre angles 0 and 90, 22½ and 112½, and 45 and 135 degrees

set by Tsai and Wu, and the failure surface becomes open-ended or hyperboloid. Ashkenazi's formulation does reduce to the Tsai and Wu form using 45 degree off-axis uniaxial strength data when tensile and compressive strengths are equal.

Puppo and Evensen (4) introduced the interaction factor $\gamma = (3S^2/XY)^n$, a measure of the material's strength anisotropy, into Hill's basic theory, and the influence of this factor on the test material's fatigue failure ellipse (10^5 cycles) for loading with the principal stresses aligned with the fibres is shown in Fig. 2. If the interaction exponent, n, is considered to be unity, $\gamma = 0.188$, and the resulting failure surface tends towards the form of the maximum stress rectangle. Correlation with the experimental data is poor. But if n is selected to give the best fit, i.e., $n = 0.5$ and, therefore, $\gamma = 0.433$, then correlation seems good except for the high positive load ratios.

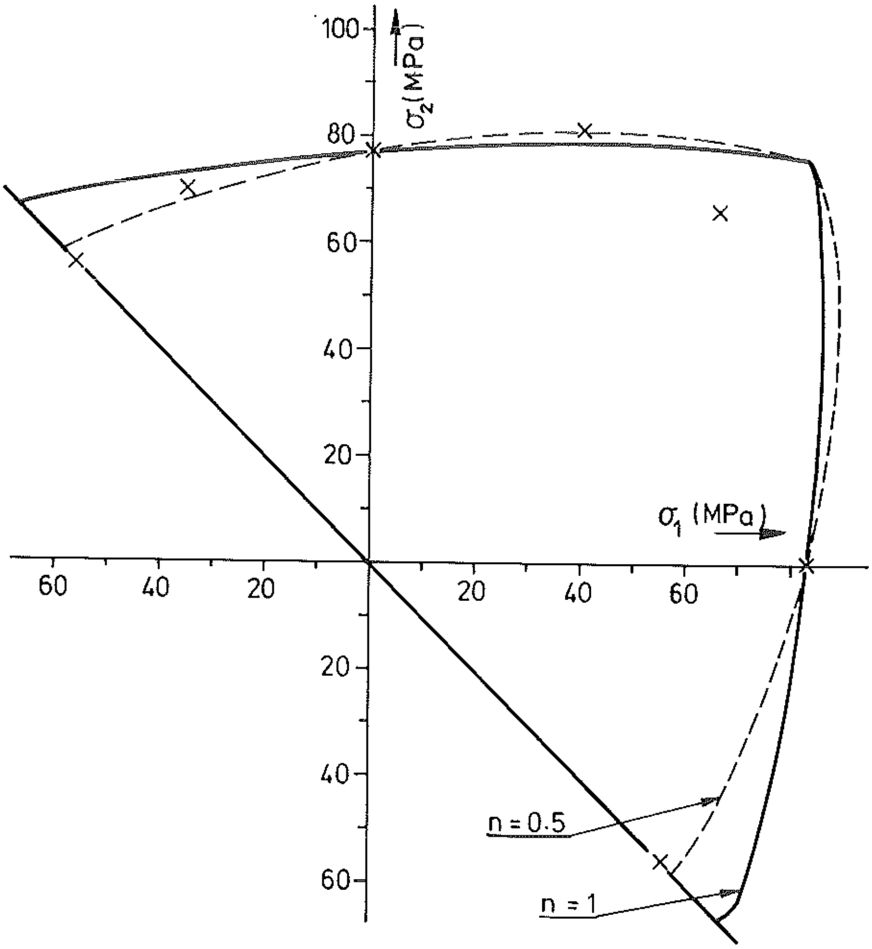

Fig 2 Failure envelopes for fatigue failure at 10^5 cycles based on the criterion of Puppo and Evensen (4) for principal load axes aligned with the fibre weave (see Appendix 2)

Monotonic failure

For the test laminate, the marked difference between tensile and compressive strengths means that those criteria which do not account for such differences are completely inadequate when applied to monotonic loading.

In Fig. 3(a)–(c), the failure ellipses according to the theories of Hoffman and of Tsai and Wu using, firstly, the equibiaxial tensile strength, and then the 45 degree shear strength, to derive F_{12} are shown. Evaluation of F_{12} by Tsai and Hahn's simplified approach gives $F_{12} = -0.970 \times 10^{-5}$ which is little different from using Hoffman's criteria ($F_{12} = -0.922 \times 10^{-5}$). Undoubtedly, if the theory of Puppo and Evensen (**4**) is modified to account for the differences in tensile and compressive strengths it shows the best fit to the test data (see Fig. 3(d)). However, this requires the optimum selection of the exponent n. Under fatigue loading the optimum value was 0.5, but for monotonic loading a value of $n = 1.67$ gives the optimum fit. There is no qualitative means of fixing n and its value is not solely dependent on the material.

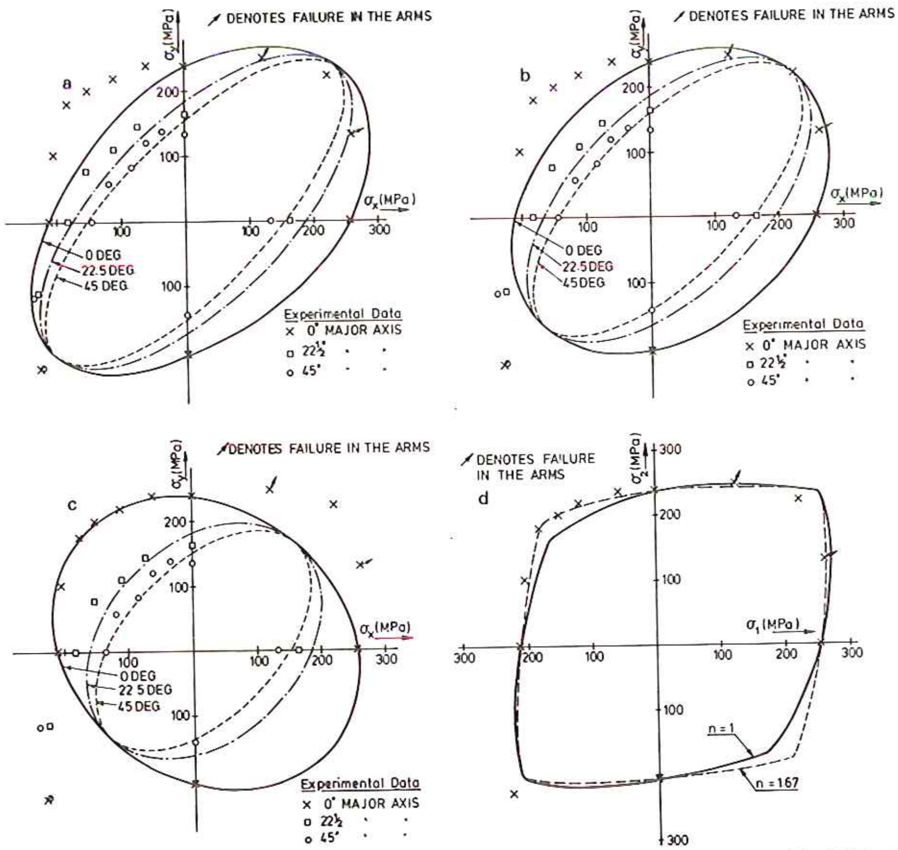

Fig 3 Failure envelopes for monotonic failure based on the theories of (a) Hoffman (22), (b) Tsai and Wu (3) with equibiaxial tensile strength, (c) Tsai and Wu (3) with 45 degree shear strength, and (d) Puppo and Evensen (4) (see Appendix 2)

Consideration of the criteria

Comparison of all the available failure criteria with experimental data shows that they are inadequate for the test laminate under consideration. The shape of the failure surface as derived for any one criterion depends on which data are used to establish the strength constants or tensors and the surface will show only reasonable fit to experimental data in the quadrant which contains the applied complex strength data. In other quadrants the correlation between the failure theory and practice can be very poor. It was shown in Part I that different failure mechanisms exist for different complex loading states and, unless each mechanism can be described by the same concept, an optimum fit over the whole failure surface may never be found. In the case of the tensor-based theories and the earlier theories from which they were evolved all mechanisms are described by distortional energy. Careful observation of progressive damage under fatigue loading has shown that the concepts of strain energy and maximum shear stress rather than distortional energy give best results. In the next section, a theory is proposed based on the interaction of strain energy and maximum shear stress.

A new theory

In Part I were outlined three progressive mechanisms of fatigue failure for the test laminate under zero mean stress cyclic loading.

(i) *Rectilinear cracking*, delamination, and, finally, lamina instability causing failure in compression.
(ii) *Shear deformation* along the plane of the fibres causing breakdown of the fibre-matrix bond.
(iii) *Combined rectilinear cracking and matrix shear deformation* on the fibre plane.

When the fibre axes and the principal stress axes coincide, then only the rectilinear cracking mechanism of failure is evident. Matrix cracking is perpendicular and, to a lesser degree parallel, to the major principal stress, and even for a load ratio of -1 there are no apparent signs of in-plane shear.

In the unique off-axis loading case of $\lambda = -1$ with 45 and 135 degree principal stress axes the maximum in-plane shear stress is coincident with the fibre plane and there are no in-plane normal stresses acting on the fibres. Then the failure mechanism is one of pure shear along the fibre plane. However, for all other off-axis loading cases there appears to be a combined mechanism of rectilinear cracking and matrix shear. Though each mechanism varies in extent with load ratio, some variation is evident also when the principal in-plane stress direction is rotated so as to vary the proportion of normal stress and in-plane shear acting on the fibre plane.

Each mechanism or progressive mode of fatigue damage under different biaxial loading and weave directions was recognised, in the first instance, by physical observation of tests at high stress levels. At low stress levels little physical damage appears in the first cycle, but with cycling the accumulation of rectilinear cracking or shear degradation and whitening can be identified. However, more direct means of corroborating the failure mode are evident from the cyclic stress/strain behaviour. The rectilinear cracking/delamination mode of failure is characterised by the following.

(1) A distinct 'knee' in the tensile half cycle of the 1st cycle stress/strain loop which disappears on subsequent loading.
(2) A linear stress/strain relationship in the compressive half cycle of the stress/strain loop.
(3) Little or no hysteresis in the cyclic stress/strain loop even at very high stress levels.
(4) A progressive build up in strain range in zero mean stress, constant stress range loading, which is almost entirely confined to the tensile range until the start of the tertiary phase. The consequence is a stress/strain loop which is distinctly crooked.
(5) A fatigue life and cyclic stress/strain behaviour which is not affected by frequency or rest periods at least in the frequency range 0.01 to 1 Hz.

The shear deformation mode is characterised by the following.

(1) A stress/strain curve showing a low yield point irrespective of the sign of the principal stresses.
(2) A true yield point which does not disappear in the second or subsequent cycles so that the stress/strain loop shows marked hysteresis.
(3) A progressive build up in principal strain range under zero mean stress loading which accumulates equally in both the tensile and compressive half cycles.
(4) A fatigue life and cyclic stress/strain behaviour which are markedly dependent on cyclic frequency and rest periods in the frequency range 0.005–1 Hz.

Though a quantitative study of rectilinear cracking was not made, the appearance and accumulation of cracks seemed to be related to strength. No plane strain condition was tested when loading along the fibre axes, but the nearest condition of $\lambda = +\frac{1}{2}$ showed the highest fatigue strength for all loading conditions. The lowest fatigue strength for principal stresses coincident with the fibre axes was for $\lambda = -1$. The equibiaxial loading condition, though resulting in rectilinear cracking along both fibre axes, did not show as much cracking as for $\lambda = -1$. This is because, under the latter condition, rather than a shear mode of failure being induced, the Poisson strain 'works with' the principal strains to accelerate cracking and delamination. With the above observations in mind, a strain energy criterion is proposed for fatigue loading along the fibre axes. The strain energy at the stress level for a definite fatigue life, i.e.

$$U_F = \frac{1}{2}\left\{\frac{\sigma_1^2}{E_1} - \left(\frac{\nu_{12}}{E_1} + \frac{\nu_{21}}{E_2}\right)\sigma_1\sigma_2 + \frac{\sigma_2^2}{E_2}\right\} \tag{4}$$

is a constant.

The extent of matrix/fibre shear degradation is dictated by the level of shear stress acting along the fibre plane. The stress conditions of pure shear acting along this plane determines the matrix/fibre shear strength. A maximum shear stress criterion is proposed. The failure strength by fibre/matrix shear for a definite fatigue life is found from the unique case of $\lambda = -1$ with 45 and 135 degree principal stress axes. This test condition is the only one which does not involve some rectilinear cracking; it is the only test condition where no component of normal stress acts along the fibre plane. By deduction, this stress state must cause the lowest equivalent strength for the composite.

Failure will be due to both rectilinear cracking and fibre/matrix shear for all off-axis loading conditions, other than the unique case of $\lambda = -1$ with 45 and 135 degree principal stress axes. For the general loading case a simple quadratic failure relationship is proposed

$$\frac{1}{\sigma_F^2} = \frac{1}{\sigma_{uF}^2} + \frac{1}{\sigma_{\tau F}^2} \tag{5}$$

where σ_F is the failure strength, i.e., the amplitude or semi range of the major principal stress. σ_{uF} is the major principal stress for the same loading condition, i.e., same values of λ and θ, which would cause failure solely by rectilinear cracking, i.e., as given by the total strain energy theory. $\sigma_{\tau F}$ is the major principal stress for the same loading condition which would cause failure solely by shear along the fibre planes, i.e., would give the same shear stress on the fibre plane as gives failure for the $\lambda = -1$, $\theta = 45$ degrees case.

In applying the criterion to the general loading case, the applied principal stress σ and $\lambda\sigma$ must be resolved as:

(1) tensile stresses normal to the fibre plane, i.e.

$$\sigma_f = \tfrac{1}{2}\sigma\{(1 + \lambda) \pm (1 - \lambda)\cos 2\theta\} \tag{6}$$

(2) shear stresses along the fibres, i.e.

$$\tau_f = \tfrac{1}{2}\sigma(1 - \lambda)\sin 2\theta \tag{7}$$

where θ is the off-axis angle. Whenever σ is such that the combined influence of the resolved components σ_f and τ_f acting on the fibre planes exceeds the condition set by equation (5), failure will occur.

The strain-energy/shear interaction theory applied to fatigue failure

The contribution of each mode of failure with different off-axis angles and load ratios is shown graphically in Fig. 4 for the particular case of fatigue failure in 10^5 cycles.

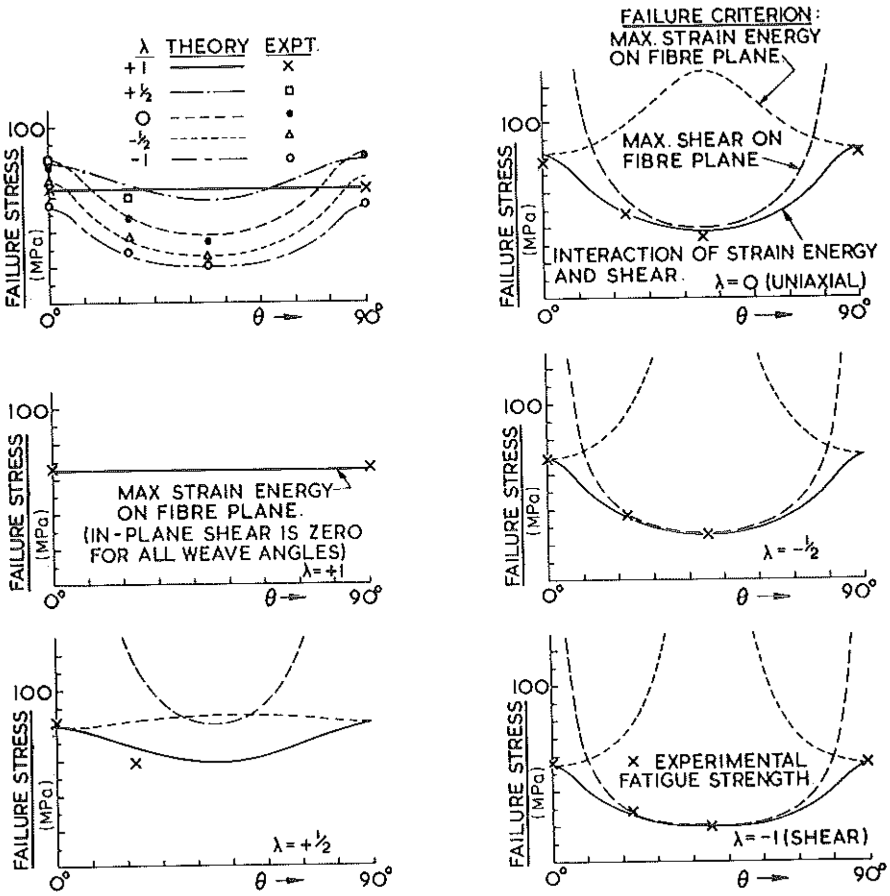

Fig 4 The contribution of rectilinear cracking and fibre/matrix shear degradation on the fatigue failure strength at 10^5 cycles based on the hypothesis of strain energy/shear interaction on the fibre plane

For equibiaxial loading no shear occurs in the fibre plane. Failure is independent of fibre angle and is described solely by total strain energy.

Off-axis loading and decreasing λ result in shear degradation along the fibre plane, the contribution increases with increasing off-axis angle and decreasing λ. But for $\lambda = +\frac{1}{2}$, only at high off-axis angles (37–53 degrees) does the shear degradation mode contribute more towards failure than does rectilinear cracking. However, any uniaxial loading ($\lambda = 0$) with off-axis angles between 14 and 76 degrees results in more shear degradation than rectilinear cracking, and for the 45 degree off-axis extreme the extent of shear degradation far outweighs that due to the cracking mode: the failure strength is calculated to be 38 MPa,

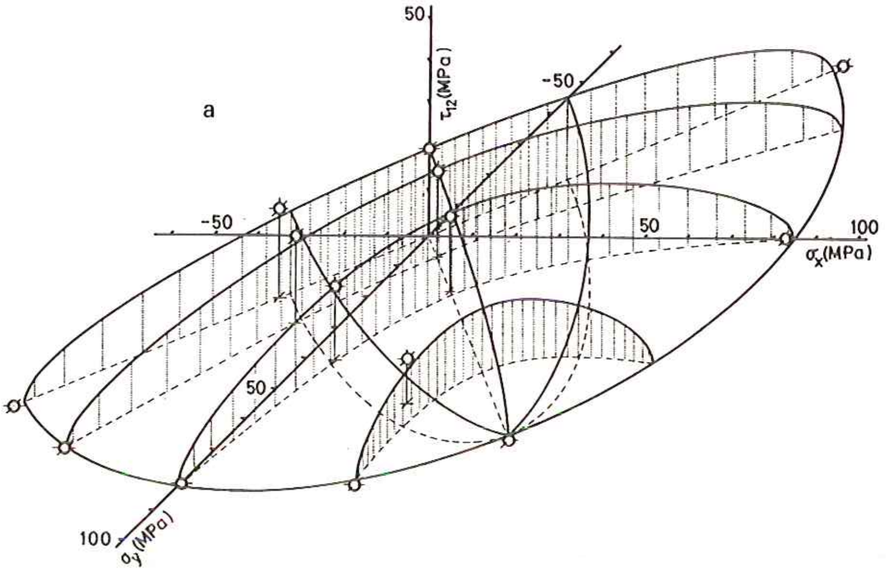

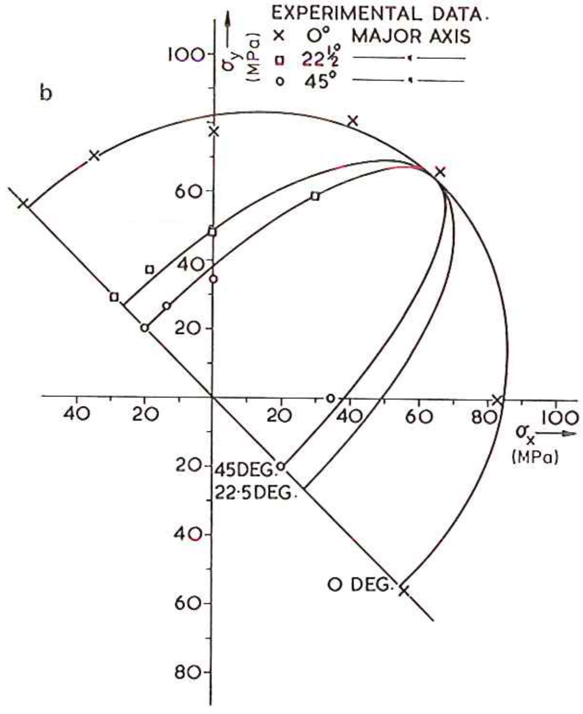

Fig 5 Failure envelopes and surfaces for fatigue at 10^5 cycles based on strain energy/shear interaction on the fibre plane. (a) True failure surfaces plotted on 3-D axes. (b) Representation as failure lines on 2-D axes

but if failure were solely due to shear degradation the strength would be 40 MPa, and if caused solely by rectilinear cracking it would be 130 MPa.

For negative load ratios, particularly $\lambda = -1$, the dominance of fibre/matrix shear is evident, and only for small off-axis angles does rectilinear cracking play a significant part. For example, an off-axis angle of 10 degrees and $\lambda = -1$ gives a failure strength of 41 MPa, whereas, if failure were due solely to shear degradation or rectilinear cracking, the strength would be 58 MPa: but if the off-axis angle were reduced to 5 degrees, the failure strength would increase to 50 MPa, as the contribution of the damaging shear mode would be less; failure solely due to shear would then give a strength of 115 MPa, and for failure exclusively due to rectilinear cracking the strength would be 56 MPa. Figure 5 shows the failure surface for a fatigue life of 10^5 cycles. The agreement with the experimental data is good, except for the case of $\lambda = +\frac{1}{2}$ with $22\frac{1}{2}$ and $112\frac{1}{2}$ degree principal stress axes. $22\frac{1}{2}$ and $112\frac{1}{2}$ asymmetric off-axis loading, in particular for positive load ratios, shows a larger growth in fibre/matrix shear deformation than expected. The extent of this exaggerated shear damage is now reflected in the low experimental strength for $\lambda = +\frac{1}{2}$. Pagano and Halpin (23) showed that, under off-axis loading, end effects could influence failure, due to restrictions caused by the grips, and Rizzo (24) felt that end constraint could have significant effect if the uniaxial specimen length/width ratio was less than 10. Although the unconstrained length/width ratio of the uniaxial test specimens was only 1.13, there was no evidence of any tendency towards grip rotation. However, the constraint caused by gripping of the biaxial cruciform specimens was almost total due to the necessity of using bonded aluminium reinforcement tabs of adequate length to prevent premature failure of the arms. Unfortunately this constraint is a consequence of using small cruciform specimens, and unless grips are employed which allow free rotation, which restricts the tests to tensile loading, a much larger test machine in terms of both physical size and load capacity must be used.

The strain energy/shear interaction theory applied to monotonic failure

For fatigue loading the correlation between the proposed theory and experiment is good, but for monotonic loading the theory proves to be less adequate. In applying the theory to monotonic failure the sign of loading was taken into account for stresses normal to the fibres, whereas the matrix/fibre shear component of strength was assumed independent of the sign of shear stress. The monotonic failure surface is shown in Fig. 6, and generally is conservative, though it does provide a better all-round fit to the experimental data of each quadrant than the tensor-based theories using either equibiaxial or 45 degree shear strengths.

The greatest discrepancy between experiment and theory was in the third quadrant, or for compression–compression loading. In this quadrant failure appears to tally best with a maximum stress criterion, but to make such an

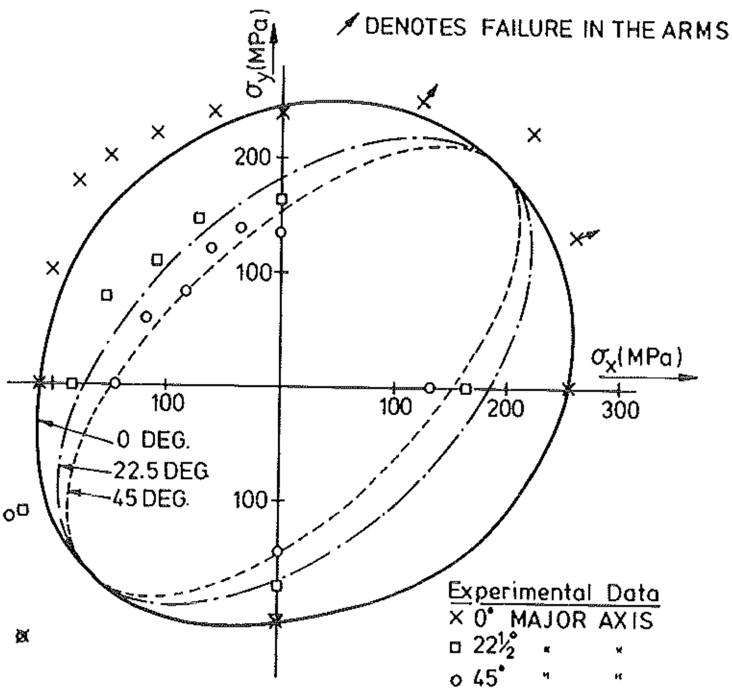

Fig 6 Failure envelopes for monotonic failure based on strain energy/shear interaction on the fibre plane

assertion from only eight compression–compression biaxial tests is merely speculation. These eight tests and one zero-compression fatigue test did not make possible any judgement on the viability of a strain energy criterion as the only progressive damage detected prior to final collapse was delamination. But, remembering the difficulties encountered in finding the true compressive strength of metals, e.g. (**25**), the question arises as to the effect of through-thickness grip constraint on the initiation and progression of delamination in biaxial compression. Certainly, under uniaxial compressive loading, wedge-type grips result in greater strengths than if compression is applied directly to the ends of the specimen through flat platens (**26**).

Prediction of the stress/strain 'knee' and off-axis yield

Formerly, the classical theories for complex loading of metals were concerned with predicting yield rather than ultimate failure. Deviation from stress/strain linearity in the woven roving test grp can be through either the 'knee' or a true yield point; each occurs due to different mechanisms, so that no single conventional 'yield' theory will predict both the stress level of the 'knee' and the off-axis yield. However, the proposed strain energy/shear theory derives two

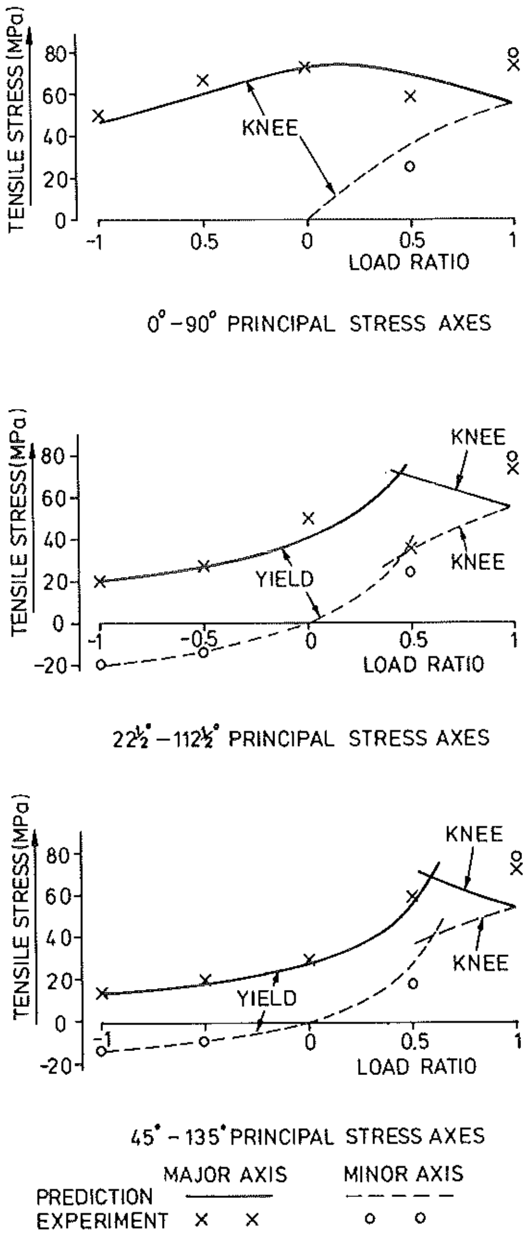

Fig 7 Prediction of the 'knee' and 'yield' based on strain energy/shear interaction on the fibre plane. Basis of prediction: (a) stress at 'knee' from total strain energy normal to the fibre plane (based on 'knee' at 72 MPa for uniaxial loading along 90 degree fibre axis); (2) yield point from shear stress along the fibre plane (based on yield at 14 MPa for shear loading, $\lambda = -1$ with 45 and 135 degree axes)

strengths independently: one is based on rectilinear cracking, which in itself is a cause of the tensile 'knee' when the principal stresses are aligned with the fibre axes, and the other strength is based on shear of the matrix, which is a yield phenomenon. If the two strengths are considered separately and the interaction quadratic is not applied, then the lower of the two will predict the limit of stress/strain proportionality. It must be borne in mind that rectilinear cracking and the 'knee' never occur if the normal stress is compressive and then the strain energy based strength is ignored.

Predictions of the 'knee' and yield point for load ratios of −1 (shear) to +1 (equibiaxial) are shown in Fig. 7 for principal stress axes of 0 and 90, $22\frac{1}{2}$ and $112\frac{1}{2}$, and 45 and 135 degrees. The major principal stress in each case is tensile.

When λ is positive and the principal stress axes are aligned with the fibres, the 'knee' appears along both minor and major load axes, and if λ is less than $+\frac{1}{2}$ a 'knee' will in fact occur along the minor principal axes *before* one appears on the major axis. Off-axis loading with a high positive load ratio still shows a 'knee', but as the off-axis angle increases, so the load ratio to cause a 'knee' becomes more positive. For $22\frac{1}{2}$ and $112\frac{1}{2}$ degree off-axis loading a 'knee' should occur along both fibre axes when λ is greater than 0.44, and for 45 and 135 degree loading the yield changes to a 'knee' at $\lambda = 0.59$. The change from a 'knee' to a yield point is not distinct because the two phenomena will intermingle (see, e.g., Fig. 4(c) of Part I) for $\lambda = +\frac{1}{2}$ and 45 and 135 degree axes).

Conclusions

A methodical study of the progressive failure mechanisms in a woven roving grp has led to the proposal of a new theory based on the interaction of rectilinear cracking and shear of the fibre/matrix interface. The former is described by consideration of strain energy due to stresses normal to the fibres, and the latter by the maximum shear aligned with the fibre-plane. Failure is represented by a simple quadratic expression. The theory is seen to describe reasonably the failure surface of the test grp under zero mean-stress fatigue loading and, less reasonably, monotonic loading. It also proved suitable for predicting the change in stress level of the 'knee'' and the yield point under biaxial loading.

Appendix 1 Anisotropic failure criteria for application to laminate materials of orthogonal symmetry

(1) Criteria which do not account for differences in tensile and compressive strengths:

(a) *Hill* (2)

$$\left(\frac{\sigma_1}{X}\right)^2 - \left(\frac{1}{X^2} + \frac{1}{Y^2} - \frac{1}{Z^2}\right)\sigma_1\sigma_2 + \left(\frac{\sigma_2}{Y}\right)^2 + \left(\frac{\tau_{12}}{S}\right)^2 = 1$$

(b) *Norris and McKinnon* (27)

$$\left(\frac{\sigma_1}{X}\right)^2 + \left(\frac{\sigma_2}{Y}\right)^2 + \left(\frac{\tau_{12}}{S}\right)^2 = 1$$

(c) *Norris* (28)

$$\left(\frac{\sigma_1}{X}\right)^2 - \frac{\sigma_1\sigma_2}{XY} + \left(\frac{\sigma_2}{Y}\right)^2 + \left(\frac{\tau_{12}}{S}\right)^2 = 1$$

(d) *Azzi and Tsai* (29)

$$\left(\frac{\sigma_1}{X}\right)^2 - \frac{\sigma_1\sigma_2}{X^2} + \left(\frac{\sigma_2}{Y}\right)^2 + \left(\frac{\tau_{12}}{S}\right)^2 = 1$$

(e) *Fischer* (30)

$$\left(\frac{\sigma_1}{X}\right)^2 - K\left(\frac{\sigma_1\sigma_2}{XY}\right) + \left(\frac{\sigma_2}{Y}\right)^2 + \left(\frac{\tau_{12}}{S}\right)^2 = 1$$

where

$$K = \frac{E_1(1 + \nu_{21}) + E_2(1 + \nu_{12})}{2\{E_1E_2(1 + \nu_{12})(1 + \nu_{21})\}^{1/2}}$$

(2) Criteria which do account for differences in tensile and compressive strengths and also require complex stress data:

(f) *Hoffman* (22)

$$\left(\frac{X' - X}{XX'}\right)\sigma_1 + \left(\frac{Y' - Y}{YY'}\right)\sigma_2 + \frac{\sigma_1^2}{XX'} - \frac{\sigma_1\sigma_2}{XX'} + \frac{\sigma_2^2}{YY'} + \frac{\tau_{12}^2}{S^2} = 1$$

(g) *Marin* (31)

$$\left(\frac{X' - X}{XX'}\right)\sigma_1 + \left(\frac{1}{Y} - \frac{Y}{XX'}\right)\sigma_2 + \left\{\frac{2}{XX'} - \frac{X'X - S(X' - X - X'X/Y' + Y)}{XX'S^2}\right\}\sigma_1\sigma_2 + \frac{\sigma_1^2}{XX'} + \frac{\sigma_2^2}{XX'} = 1$$

(h) *Franklin* (32)

$$\left(\frac{X' - X}{XX'}\right)\sigma_1 + \left(\frac{Y' - Y}{YY'}\right)\sigma_2 + \frac{\sigma_1^2}{XX'} - \frac{\overline{K}_2\sigma_1\sigma_2}{XX'} + \frac{\sigma_2^2}{YY'} + \frac{\tau_{12}^2}{S^2} = 1$$

$\bar{K}_2$ acts as a distorting factor for each quadrant of the failure boundary. For example the equibiaxial tension case gives

$$\bar{K}_2 = 1 + \frac{XX'}{YY'} + \frac{1}{EQ}\left\{(X' - X) + (Y' - Y)\frac{X'X}{Y'Y}\right\} - \frac{X'X}{EQ^2}$$

(3) Criteria which are presented in tensorial form, and generally are adaptable to take optimum or experimentally available complex stress data

(i) *Gol'denblat and Kopnov* (**5**)

$$\left(\frac{1}{X} - \frac{1}{X'}\right)\frac{\sigma_1}{1} + \left(\frac{1}{Y} - \frac{1}{Y'}\right)\frac{\sigma_2}{2} + \left[\left(\frac{1}{X} + \frac{1}{X'}\right)^2\left(\frac{\sigma_1}{2}\right)^2 + \left(\frac{1}{Y} + \frac{1}{Y'}\right)^2\left(\frac{\sigma_2}{2}\right)^2 + \left\{\left(\frac{1}{X} + \frac{1}{X'}\right) + \left(\frac{1}{Y} + \frac{1}{Y'}\right)^2 - \left(\frac{1}{S^+_{45}} + \frac{1}{S^-_{45}}\right)^2\right\} \times \frac{\sigma_1\sigma_2}{8} + \left(\frac{1}{S^+} + \frac{1}{S^-}\right)^2\left(\frac{\tau_{12}}{4}\right)^2\right]^{1/2} = 1$$

(j) *Ashkenazi* (**6**)

$$\left(\frac{\sigma_1}{X}\right)^2 + \left(\frac{\sigma_2}{Y}\right)^2 + \left(\frac{4}{W^2} - \frac{1}{X^2} - \frac{1}{Y^2} - \frac{1}{S^2}\right)\sigma_1\sigma_2 + \left(\frac{\tau_{12}}{S}\right)^2 = 1$$

(k) *Tsai and Wu* (**3**)

A generalised 4th order tensor criterion

$$F_1\sigma_1 + F_2\sigma_2 + F_6\sigma_6 + F_{11}\sigma_1^2 + 2F_{12}\sigma_1\sigma_2 + F_{22}\sigma_2^2 + F_{66}\sigma_6^2 = 1$$

where

$$F_1 = \frac{1}{X} - \frac{1}{X'}; \qquad F_2 = \frac{1}{Y} - \frac{1}{Y'}; \qquad F_6 = \frac{1}{S^+} - \frac{1}{S^-}$$

$$F_{11} = \frac{1}{XX'}; \qquad F_{22} = \frac{1}{YY'}; \qquad F_{66} = \frac{1}{S^+S^-}$$

F_{12} can be determined from a range of strengths, e.g., (i) from the equibiaxial tensile strength, EQ

$$F_{12} = \frac{1}{2EQ^2}\left\{1 - EQ\left(\frac{1}{X} - \frac{1}{X'} + \frac{1}{Y} - \frac{1}{Y'}\right) - EQ^2\left(\frac{1}{XX'} - \frac{1}{YY'}\right)\right\}$$

(ii) from the 45 degree off-axis uniaxial strength, W and the shear strength, S

$$F_{12} = \frac{2}{W^2}\left\{1 - \frac{W}{2}\left(\frac{1}{X} - \frac{1}{X'} + \frac{1}{Y} - \frac{1}{Y'}\right) - \frac{W^2}{4}\left(\frac{1}{XX'} + \frac{1}{YY'} + \frac{1}{S^2}\right)\right\}$$

or (iii) from the shear strength at 45 degrees to the orthogonal axes, S_{45}

$$F_{12} = -\frac{1}{2S_{45}^2}\left\{1 - S_{45}\left(\frac{1}{X} - \frac{1}{X'} + \frac{1}{Y} - \frac{1}{Y'}\right) - S_{45}^2\left(\frac{1}{XX'} + \frac{1}{YY'}\right)\right\}$$

(l) *Wu and Scheublein* (7)

A generalised 6th order tension criterion

$$F_1\sigma_1 + F_2\sigma_2 + F_{11}\sigma_1^2 + F_{22}\sigma_2^2 + F_{66}\sigma_6^2 + F_{12}\sigma_1\sigma_2 + F_{112}\sigma_1^2\sigma_2 + F_{122}\sigma_1\sigma_2^2 + F_{166}\sigma_1\sigma_6^2 + F_{266}\sigma_2\sigma_6^2 = 1$$

The first five components are the same as in the Tsai and Wu criterion above, but the remaining five must be obtained by iteration.

(m) *Puppo and Evensen* (4)

1st criterion

$$\left(\frac{\sigma_1}{X}\right)^2 - \gamma\left(\frac{\sigma_1\sigma_2}{Y^2}\right) + \gamma\left(\frac{\sigma_2}{Y}\right)^2 + \left(\frac{\tau_{12}}{S}\right)^2 = 1$$

2nd criterion

$$\gamma\left(\frac{\sigma_1}{X}\right)^2 - \gamma\left(\frac{\sigma_1\sigma_2}{X^2}\right) + \left(\frac{\sigma_2}{Y}\right)^2 + \left(\frac{\tau_{12}}{S}\right)^2 = 1$$

where the interaction factor,

$$\gamma = \left(\frac{3S^2}{XY}\right)^n$$

and the exponent, n, depends on the material.

APPENDIX 2

(1) Application to monotonic failure

Theory of Puppo and Evensen (see Fig. 2)

1st criterion

$$\left(\frac{\sigma_1}{X}\right)^2 - \gamma\left(\frac{\sigma_1\sigma_2}{Y^2}\right) + \gamma\left(\frac{\sigma_2}{Y}\right)^2 + \left(\frac{\tau_{12}}{S}\right)^2 = 1$$

2nd criterion

$$\gamma\left(\frac{\sigma_1}{X}\right)^2 - \gamma\left(\frac{\sigma_1\sigma_2}{X^2}\right) + \left(\frac{\sigma_2}{Y}\right)^2 + \left(\frac{\tau_{12}}{S}\right)^2 = 1$$

where the interaction factor

$$\gamma = \left(\frac{3S^2}{XY}\right)^n$$

and the exponent n depends on the material. For $n = 1$, $\gamma = 0.188$, giving strength tensors

1st criterion	*2nd criterion*
$F_{11} = \frac{1}{X^2} = 0.1452 \times 10^{-3}$	$F_{11} = \frac{\gamma}{X^2} = 0.2730 \times 10^{-4}$
$F_{22} = \frac{\gamma}{Y^2} = 0.3172 \times 10^{-4}$	$F_{22} = \frac{1}{Y^2} = 0.1687 \times 10^{-3}$
$F_{12} = -\frac{\gamma}{2Y^2} = 0.1586 \times 10^{-4}$	$F_{12} = \frac{1}{2X^2} = -0.1365 \times 10^{-4}$

Best fit is found for $n = 0.5$, then $\gamma = 0.433$ gives strength tensors

1st criterion	*2nd criterion*
$F_{11} = 0.1452 \times 10^{-3}$	$F_{11} = 0.6287 \times 10^{-4}$
$F_{22} = 0.7305 \times 10^{-4}$	$F_{22} = 0.1687 \times 10^{-3}$
$F_{12} = 0.3652 \times 10^{-4}$	$F_{12} = 0.3144 \times 10^{-4}$

(2) Application to fatigue failure

Theory of Hoffman (see Fig. 3)

$$\left(\frac{1}{X} - \frac{1}{X'}\right)\sigma_1 + \left(\frac{1}{Y} - \frac{1}{Y'}\right)\sigma_2 + \frac{\sigma_1^2}{XX'} - \frac{\sigma_1\sigma_2}{XX'} + \frac{\sigma_2^2}{YY'} + \left(\frac{\tau_{12}}{S}\right)^2 = 1$$

F_1	$= -0.8483 \times 10^{-3}$
F_2	$= -0.6527 \times 10^{-3}$
F_{11}	$= 0.1844 \times 10^{-4}$
F_{22}	$= 0.2040 \times 10^{-4}$
F_{12}	$= -0.9220 \times 10^{-5}$
F_{66}	$= 0.1452 \times 10^{-3}$

Tsai and Wu: F_{12} *from equibiaxial tension (see Fig. 3)*

$$F_1\sigma_1 + F_2\sigma_2 + F_{11}\sigma_1^2 + 2F_{12}\sigma_1\sigma_2 + F_{22}\sigma_2^2 + F_{66}\sigma_6^2 = 1$$

$$F_1 = \frac{1}{X} - \frac{1}{X'} = -0.8483 \times 10^{-3}$$

$$F_2 = \frac{1}{Y} - \frac{1}{Y'} = -0.6527 \times 10^{-3}$$

$$F_{11} = \frac{1}{XX'} = 0.1844 \times 10^{-4}$$

$$F_{22} = \frac{1}{YY'} = 0.2040 \times 10^{-4}$$

$$F_{66} = \frac{1}{S^2} = 0.1452 \times 10^{-3}$$

$$F_{12} = \frac{1}{2EQ^2}\left\{1 - EQ\left(\frac{1}{X} - \frac{1}{X'} + \frac{1}{Y} - \frac{1}{Y'}\right) - EQ^2\left(\frac{1}{XX'} - \frac{1}{YY'}\right)\right\} = -0.5999 \times 10^{-5}$$

where EQ is the equibiaxial tensile strength.

Tsai and Wu: F_{12} *from 45 degree shear (see Fig. 3)*

$$F_1\sigma_1 + F_2\sigma_2 + F_{11}\sigma_1^2 + 2F_{12}\sigma_1\sigma_2 + F_{22}\sigma_2^2 + F_{66}\sigma_6^2 = 1$$

Strength tensors F_1, F_2, F_{11}, F_{22}, and F_{66} same as above.

$$F_{12} = -\frac{1}{2S_{45}^2}\left\{1 - S_{45}\left(\frac{1}{X} - \frac{1}{X'} - \frac{1}{Y} + \frac{1}{Y'}\right) - S_{45}^2\left(\frac{1}{XX'} + \frac{1}{YY'}\right)\right\}$$
$$= 0.3617 \times 10^{-5}$$

where S_{45} is the shear strength along a plane at 45 degrees to the fibres.

Puppo and Evensen (see Fig. 3)

Failure quadrant	γ	
	n = *1*	n = *1.67*
1st	0.338	0.163
2nd	0.390	0.208
3rd	0.475	0.289
4th	0.412	0.227

References

(1) NORRIS, C. B. (1939) The elastic theory of wood failure, *Trans Am. Soc. mech. Engrs*, **61**, 251–261.

(2) HILL, R. (1948) A theory of yielding and plastic flow of anisotropic metals, *Proc. Roy. Soc. Lond., Ser. A*, **193**, 281–297.

(3) TSAI, S. W. and WU, E. M. (1971) A general theory of strength for anisotropic materials, *J. Composite Mater.*, **5**, 58–80.

(4) PUPPO, A. H. and EVENSEN, H. A. (1967) Strength of anisotropic materials under combined stresses, *JAIAA*, **10**, 468–474.

(5) GOL'DENBLAT, I. I. and KOPNOV, V. A. (1965) Strength of glass reinforced plastics in the complex stress state, *Mekhanika Polimerov*, **1**, 70–78.

(6) ASHKENAZI, E. K. (1965) Problems of the anisotropy of strength. *Mekhanika Polimerov*, **1**, 79–92.

(7) WU, E. M. and SCHEUBLEIN, J. K. (1974) Laminate strength – a direct characterisation procedure, *Composite Materials: Testing and Design* (3rd Conf.), *ASTM STP 546*, ASTM, Philadelphia, PA, pp. 188–206.

(8) WU, E. M. (1972) Optimal experimental measurement of anisotropic failure tensors, *J. Composite Mater.*, **6**, 472–489.

(9) OWEN, M. J. and FOUND, M. S. (1972) Static and fatigue failure of glass reinforced polyester resins under complex stress conditions, *Faraday Special Discussions of the Chemical Society No. 2*, pp. 77–89.

(10) OWEN, M. J. and GRIFFITHS, J. R. (1978) Evaluation of biaxial stress fatigue failure surfaces for a glass reinforced polyester resin under static and fatigue loading, *J. Mater. Sci.*, **13**, 1521–1537.

(11) OWEN, M. J. and RICE, D. J. (1982) Biaxial strength behaviour of glass-reinforced polyester resins, *Composite Materials: Testing and Design* (6th Conf.), *ASTM STP 787*, ASTM, Philadelphia, PA, pp. 124–144.

(12) TENNYSON, R. C., MACDONALD, D., and NANYARO, A. P. (1978) Evaluation of the tensor polynomial failure criterion for composite materials, *J. Composite Mater.*, **12**, 63–75.

(13) NARAYANASWAMI, R. and ADELMAN, H. M. (1977) Evaluation of the tensor polynomial and the Hoffman strength theories for composite materials, *J. Composite Mater.*, **11**, 366–377.

(14) TSAI, S. W. and HAHN, H. T. (1980) *Introduction to Composite Materials*, Technomic Publishing, Westport, CT.

(15) PUCK, A. and SCHNEIDER, W. (1969) On failure mechanisms and failure criteria of filament wound glass-fibre/resin composites, *Plastics Polymers*, **37**, 33–44.

(16) SIMS, D. F. and BROGDON, V. H. (1977) Fatigue behaviour of composites under different loading modes, *Fatigue of Filamentary Composite Materials, ASTM STP 636*, ASTM, Philadelphia, PA, pp. 185–205.

(17) HASHIN, Z. and ROTEM, A. (1973) A fatigue failure criterion for fibre reinforced materials, *J. Composite Mater.*, **7**, 448–464.

(18) HASHIN, Z. (1981) Fatigue failure criteria for unidirectional fiber composites, *Trans ASME, J. Appl. Mech.*, **48**, 846–852.

(19) SANDERS, R. C., EDGE, E. C., and GRANT, P. (1983) Basic failure mechanisms of laminated composites and related aircraft design implications, *Proc. 2nd Int. Conf. on Composite Structures*, Paisley, pp. 467–485.

(20) OWEN, M. J. and FOUND, M. S. (1975) The fatigue behaviour of a glass-fabric reinforced polyester resin under off-axis loading, *J. Phys D: Appl. Phys*, **8**, 480–497.

(21) SMITH, E. W. and PASCOE, K. J. (1976) Behaviour of a glass-fibre reinforced composite subject to biaxial monotonic and fatigue loading, *Proc. 2nd Int. Conf. on Mechanical Behaviour of Materials*, Boston, pp. 941–945.

(22) HOFFMAN, O. (1967) The brittle strength of orthotropic materials, *J. Composite Mater.*, **1**, 200–206.

(23) PAGANO, N. J. and HALPIN, J. C. (1968) Influence of end constraint in the testing of anisotropic bodies, *J. Composite Mater.*, **2**, 18–31.

(24) RIZZO, R. R. (1969) More on the influence of end constraints on off-axis tensile tests, *J. Composite Mater.*, **3**, 202–219.

(25) TIMOSHENKO, S. (1941) *Strength of Materials, Part II*, Macmillan, London.
(26) FRIED, N. and WINNANS, R. R. (1963) Compressive strength of parallel filament reinforced plastics: Development of a new test method, *Standards for Filament-Wound Reinforced Plastics, ASTM STP 327*, ASTM, Philadelphia, PA, pp. 532–537.
(27) NORRIS, C. B. and McKINNON, P. F. (1956) Compression, tension and shear tests on yellow-poplar plywood panels of sizes that do not buckle with tests made at various angles to the face grain, Forest Products Laboratory, Report No. 1328.
(28) NORRIS, C. B. (1962) Strength of orthotropic materials subjected to combined stresses, Forest Products Laboratory, Report No. 1816.
(29) AZZI, V. D. and TSAI, S. W. (1965) Anisotropic strength of composites, *Expl Mech.*, **5**, 283–288.
(30) FISCHER, L. (1967) Optimisation of orthotropic laminates, *Trans. ASME Ser. B, Engng Industry*, **89**, 399–402.
(31) MARIN, J. (1957) Theories of strength for combined stresses and nonisotropic materials, *J. Aeronaut. Sci.*, **24**, 265–268, 274.
(32) FRANKLIN, H. G. (1968) Classic theories of failure of anisotropic materials, *Fibre Sci. Technol.*, **1**, 137–150.